# CAPACITY IMPROVEMENT IN UMTS BY DEDICATED RADIO RESOURCE MANAGEMENT

*Thomas Brüggen, Marc Werner, Yann Vasseur, Jochen Trenzinger and Peter Vary*

Institute of Communication Systems and Data Processing (ind)
Aachen University of Technology
{brueggen, werner, vary}@ind.rwth-aachen.de

## ABSTRACT

The IMT-2000 standard UMTS (Universal Mobile Telecommunications System) [1] is based on Wideband CDMA (Code Division Multiple Access). The service quality in terms of coverage, data rates, bit error rates, etc., and the system capacity depend on the Radio Resource Management (RRM) [1], i.e., the service-specific dynamic allocation of transmit powers, spreading factors, and codes to the individual users. In addition, macrodiversity allows "soft handoff" [2, 3] and load distribution between adjacent cells.

In this paper, two new dedicated downlink RRM functions are presented to increase the average Signal to Interference Power Ratio (SIR) and the user capacity, taking the assignment of Scrambling Codes (SC) and the power allocation in case of macrodiversity into consideration. The presented scrambling code allocation method is shown to enhance the cell capacity in a UMTS-FDD system. The improvement is derived analytically and confirmed by statistical system simulations.

For macrodiversity, a combination of power partitioning and pilot power control can increase the capacity of a single cell. The size of macrodiversity areas can be adjusted to a certain extent by these mechanisms. Thus, the power resources of less loaded cells can be exploited more efficiently.

## 1. UMTS DOWNLINK SIR CALCULATION

For a given data rate and channel coding scheme, the ratio of signal to interference power (SIR) at the receiver determines the UMTS radio link quality in terms of bit error rate. The control of transmission powers, data rates, spreading and scrambling codes is performed by the RRM to ensure that the target SIR for all connections is met.

Apart from the desired signal, each of the $N$ mobile stations $\mathrm{MS}_j$ per cell receives intra-cell interference $I_j^{\text{intra}}$ from the base station $\mathrm{BS}^0$ of its own cell and inter-cell interference $I_j^{\text{inter}}$ from base stations $\mathrm{BS}^i$ of the surrounding cells. With $P_j^0$ denoting the power fraction transmitted by $\mathrm{BS}^0$ to $\mathrm{MS}_j$ and $L_j^0$ the path loss from $\mathrm{BS}^0$ to $\mathrm{MS}_j$, the SIR at receiver $j$ is

$$\mathrm{SIR}_j = \frac{P_j^0 \cdot L_j^0}{I_j^{\text{inter}} + I_j^{\text{intra}}}, \qquad j = 1 \ldots N \tag{1}$$

We assume that each of the base stations $\mathrm{BS}^0$ and $\mathrm{BS}^i$ transmit the same power $P^0 = P^i$. The variable $\delta_j$ is defined as the ratio of inter-cell interference to the total received power from $\mathrm{BS}^0$ for user $j$, considering omnidirectional antennas and the first ring of six interfering cells:

$$\delta_j = \frac{I_j^{\text{inter}}}{P^0 \cdot L_j^0} = \sum_{i=1}^{6} \frac{P^i \cdot L_j^i}{P^0 \cdot L_j^0} = \sum_{i=1}^{6} \frac{L_j^i}{L_j^0} \tag{2}$$

The value of $\delta_j$ depends on the geographic positions of the different mobile stations and the path loss exponent $\gamma$. For $\gamma = 3.5$, $\delta_j$ takes a maximum value of $\delta_{\max} = 2.243$ at the cell border. The mean value for random uniform positions of $\mathrm{MS}_j$ is $\overline{\delta} = 0.461$ and the variance $\mathrm{var}(\delta) = 0.218$.

There are two sources of $I_j^{\text{intra}}$. The first one is a possible lack of orthogonality between the OVSF (Orthogonal Variable Spreading Factor) spreading codes due to multi-path propagation (represented by the orthogonality factor $\alpha \in [0,\ 1]$ with $\alpha = 0$ indicating full orthogonality). This part of intra-cell interference originates from transmissions employing the same scrambling code as the desired signal.

The second source of $I_j^{\text{intra}}$ is introduced if the first OVSF code tree is fully used in the radio cell, and a second OVSF tree with a different scrambling code is employed. The signals scrambled with the second code lose their orthogonality to the signals employing the first code and vice versa, and therefore fully contribute to the intra-cell interference. Assuming that $P_j^0 \ll P^0$,

$$I_j^{\text{intra}} \approx \alpha_j \cdot \sum_{\substack{k \\ \mathrm{SC}(k)=\mathrm{SC}(j)}} P_k^0 \cdot L_j^0 + \sum_{\substack{k \\ \mathrm{SC}(k)\neq\mathrm{SC}(j)}} P_k^0 \cdot L_j^0 \tag{3}$$

where $\mathrm{SC}(k)$ denotes the scrambling code used for $\mathrm{MS}_k$.

Let $\beta_j$ be the fraction of the total power $P^0$ transmitted by the base station $\mathrm{BS}^0$ to mobile stations using a scrambling code *different* from $\mathrm{SC}(j)$,

$$\beta_j = \sum_{\substack{k \\ \mathrm{SC}(k)\neq\mathrm{SC}(j)}} \frac{P_k^0}{P^0} \tag{4}$$

It follows that

$$I_j^{\text{intra}} = (\alpha_j(1-\beta_j) + \beta_j) \cdot P^0 \cdot L_j^0 \tag{5}$$

and we finally obtain

$$\mathrm{SIR}_j = \frac{P_j^0 / P^0}{\alpha_j(1-\beta_j) + \beta_j + \delta_j} \tag{6}$$

This simple SIR estimation does not include time-varying radio channel effects like fading. However, it is suitable for the analysis of the downlink scrambling code assignment in UMTS.

## 2. SCRAMBLING CODE ALLOCATION

When the number of mobile stations in one cell, $N$, and the assigned spreading factors require a second OVSF tree under a different scrambling code to be used, the question of how to allocate the two scrambling codes to the different mobile stations arises.

### 2.1. Analytical Approach

The following assumptions are made: All MSs use the same service, and power control is in equilibrium, i.e., all MSs have the same SIR value $\rho_0$,

$$\mathrm{SIR}_j \stackrel{!}{=} \rho_0 \tag{7}$$

and employ the same data rate and spreading factor (SF). Let $N > N_{\mathrm{SF}}$ with $N_{\mathrm{SF}}$ being the maximum user capacity of one OVSF tree with the SF considered. Assume there are two SCs used in the cell. Let $N_{\mathrm{I}} \geq N_{\mathrm{II}}$ be the numbers of MSs using scrambling code $\mathrm{SC_I}$ and $\mathrm{SC_{II}}$, respectively. $\beta_{\mathrm{I}}$ and $\beta_{\mathrm{II}}$, the power fractions of $P^0$ producing intra-cell interference to MSs employing scrambling code $\mathrm{SC_I}$ and $\mathrm{SC_{II}}$, respectively, can be derived from Eq. (6):

$$\beta_{\mathrm{I}} = \sum_{\substack{k \\ \mathrm{SC}(k)=\mathrm{SC_{II}}}} \frac{P_k^0}{P^0} = \rho_0 \cdot \sum_{\substack{k \\ \mathrm{SC}(k)=\mathrm{SC_{II}}}} (\alpha_k + (1-\alpha_k)\beta_{\mathrm{II}} + \delta_k) \tag{8}$$

and similarly for $\beta_{\mathrm{II}}$. This simplifies to

$$\beta_{\mathrm{I}} = \rho_0 \cdot N_{\mathrm{II}} \cdot (\overline{\alpha}_{\mathrm{II}} + \overline{\delta}_{\mathrm{II}} + (1-\overline{\alpha}_{\mathrm{II}})\beta_{\mathrm{II}}) \tag{9}$$

$$\beta_{\mathrm{II}} = \rho_0 \cdot N_{\mathrm{I}} \cdot (\overline{\alpha}_{\mathrm{I}} + \overline{\delta}_{\mathrm{I}} + (1-\overline{\alpha}_{\mathrm{I}})\beta_{\mathrm{I}}) \tag{10}$$

with $\overline{\alpha}_{\mathrm{I,\,II}}$ and $\overline{\delta}_{\mathrm{I,\,II}}$ being the mean values of $\alpha$ and $\delta$ over the MSs which employ a common $\mathrm{SC_I}$ or $\mathrm{SC_{II}}$.

Let $\overline{\epsilon_{\mathrm{I}}} = \overline{\alpha}_{\mathrm{I}} + \overline{\delta}_{\mathrm{I}}$ and $\overline{\epsilon_{\mathrm{II}}} = \overline{\alpha}_{\mathrm{II}} + \overline{\delta}_{\mathrm{II}}$. Equations 9 and 10 can be expressed as:

$$\begin{pmatrix} \beta_{\mathrm{I}} \\ \beta_{\mathrm{II}} \end{pmatrix} = \frac{\rho_0}{1-\rho_0^2 N_{\mathrm{I}} N_{\mathrm{II}}(1-\overline{\alpha}_{\mathrm{I}})(1-\overline{\alpha}_{\mathrm{II}})} \cdot \begin{pmatrix} N_{\mathrm{II}}(\overline{\epsilon_{\mathrm{II}}} + \rho_0 N_{\mathrm{I}} \overline{\epsilon_{\mathrm{I}}}(1-\overline{\alpha}_{\mathrm{II}})) \\ N_{\mathrm{I}}(\overline{\epsilon_{\mathrm{I}}} + \rho_0 N_{\mathrm{II}} \overline{\epsilon_{\mathrm{II}}}(1-\overline{\alpha}_{\mathrm{I}})) \end{pmatrix} \tag{11}$$

The constraint $\beta_{\mathrm{I}} + \beta_{\mathrm{II}} = 1$ yields a quadratic equation in $\rho_0$:

$$\rho_0^2 \cdot N_{\mathrm{I}} N_{\mathrm{II}} \cdot A + \rho_0 \cdot N\overline{\epsilon} - 1 = 0 \tag{12}$$

where

$$A = (1-\overline{\alpha}_{\mathrm{I}})(1-\overline{\alpha}_{\mathrm{II}}) + \overline{\epsilon_{\mathrm{I}}}(1-\overline{\alpha}_{\mathrm{II}}) + \overline{\epsilon_{\mathrm{II}}}(1-\overline{\alpha}_{\mathrm{I}})$$

Eq. 12 can be solved with respect to $\rho_0$:

$$\rho_0 = \frac{-N\overline{\epsilon} + \sqrt{N^2\overline{\epsilon}^2 + 4N_{\mathrm{I}}N_{\mathrm{II}} \cdot A}}{2N_{\mathrm{I}}N_{\mathrm{II}} \cdot A} \tag{13}$$

where $N\overline{\epsilon} = N_{\mathrm{I}}\overline{\epsilon_{\mathrm{I}}} + N_{\mathrm{II}}\overline{\epsilon_{\mathrm{II}}}$.

$N_{\mathrm{I}}$, $N_{\mathrm{II}}$, $\overline{\epsilon_{\mathrm{I}}}$ and $\overline{\epsilon_{\mathrm{II}}}$ should maximize the common SIR, $\rho_0$. Note that usually $\overline{\alpha}_{\mathrm{I}} \approx \overline{\alpha}_{\mathrm{II}} \approx \alpha$, so that the above expression simplifies to

$$\rho_0 = \frac{-N\overline{\epsilon} + \sqrt{N^2\overline{\epsilon}^2 + 4N_{\mathrm{I}}N_{\mathrm{II}}((1-\alpha)^2 + (1-\alpha)(\overline{\epsilon_{\mathrm{I}}} + \overline{\epsilon_{\mathrm{II}}}))}}{2N_{\mathrm{I}}N_{\mathrm{II}}((1-\alpha)^2 + (1-\alpha)(\overline{\epsilon_{\mathrm{I}}} + \overline{\epsilon_{\mathrm{II}}}))} \tag{14}$$

(the above solutions for $\rho_0$ are only valid if $A \neq 0$, i.e. $\alpha \neq 1$). Since $N\overline{\epsilon}$ is constant, $N_{\mathrm{I}}N_{\mathrm{II}}((1-\alpha)^2 + (1-\alpha)(\overline{\epsilon_{\mathrm{I}}} + \overline{\epsilon_{\mathrm{II}}}))$ must be minimized.

### 2.2. Interpretation and Simulation Results

Two rules can be derived from this solution:

**Rule 1:** The product $N_{\mathrm{I}}N_{\mathrm{II}}$ takes a small value if $N_{\mathrm{I}} \gg N_{\mathrm{II}}$. Thus, the OVSF tree under $\mathrm{SC_I}$ should be fully used and the OVSF tree under $\mathrm{SC_{II}}$ should be as unoccupied as possible.

**Rule 2:** In case of $N_{\mathrm{I}} \gg N_{\mathrm{II}}$, the term $\overline{\epsilon_{\mathrm{I}}} + \overline{\epsilon_{\mathrm{II}}}$ is minimized by the allocation of $\mathrm{SC_{II}}$ to the MSs close to the cell center, because then the inter-cell interference part in $\epsilon$ yields $\overline{\epsilon_{\mathrm{II}}} \approx \epsilon_{\min}$ and $\overline{\epsilon_{\mathrm{I}}} \approx \overline{\epsilon}$ (if $\alpha \approx$ const.).

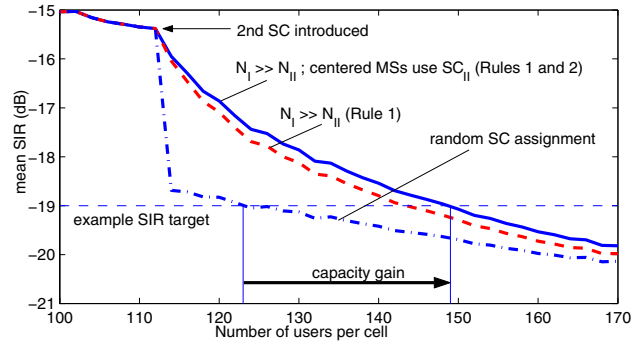


Figure 1: Scrambling code assignment strategies

The above statements remain unchanged in the case of multiple services and data rates, and are also valid in the case of fading (a general analysis of the capacity of DS/CDMA systems in a multipath fading environment is given, e.g., in [4, 5]).

In Fig. 1, the effect of these two rules on the SIR is illustrated for UMTS speech service (AMR codec, net data rates 4.75 to 12.2 kbit/s), SF=128 and perfect orthogonality ($\alpha$=0). The SIR values are based on statistical system-level simulations with randomly chosen MS positions in a hexagonal cell cluster. Six interfering neighboring cells were taken into account. The AMR mode for each connection is selected according to the SIR, which is realized by power control.

It can be observed that when the number of users exceeds the capacity of the OVSF tree for the chosen SF (one branch of the OVSF tree with SF=8 was reserved for control channels), the SIR decreases more rapidly than before due to the intra-cell interference. The lowest curve of Fig. 1 represents the case where the two SCs are assigned randomly to the MSs. As soon as the second SC is employed, approximately half of the transmissions produce intra-cell interference, causing the SIR to drop.

In the case of the two upper curves of Fig. 1, the number of MSs using $\mathrm{SC_I}$ remains at a maximum, $N_{\mathrm{I}} = N_{\mathrm{SF}}$. The additional intra-cell interference does not result in a downwards SIR step. Most MSs experience only little intra-cell interference. However, the (few) MSs employing $\mathrm{SC_{II}}$ are exposed to a large amount of interference. The transmit powers of these signals are therefore set to a relatively high level (also depending on the path loss between BS and MSs), which in turn increases the intra-cell interference to MSs using $\mathrm{SC_I}$. It is therefore beneficial if the second SC is assigned to MSs close to the cell center where the path loss is low. This effect (rule 2) is represented by the upper curve of Fig. 1.

For an example SIR target of -19 dB (corresponding to a net BER of $10^{-3}$ for AMR mode 3, channel code rate $1/2$, over an AWGN channel), the capacity in terms of active users per cell is increased by 26 when the two rules are observed (Fig. 1).

Fig. 2 illustrates the effect of increasing link quality due to selecting a higher SF, and thereby abandoning the second SC. The upper diagram shows the mean SIR values for an increasing number of MSs within a UMTS radio cell, for the case that the two SC assignment rules are observed (corresponds to upper curve of Fig. 1).

In the lower part of Fig. 2, the probabilities of chosen spreading factors and AMR modes are plotted. The SIR targets for the highest and lowest AMR modes are also indicated. A dedicated RRM algorithm was implemented to control transmission powers, AMR modes and spreading factors, so that the SIR is equal for all users. In some cases, however, it is not desirable that all MSs experience exactly the same SIR and AMR mode $n$. A slightly un-

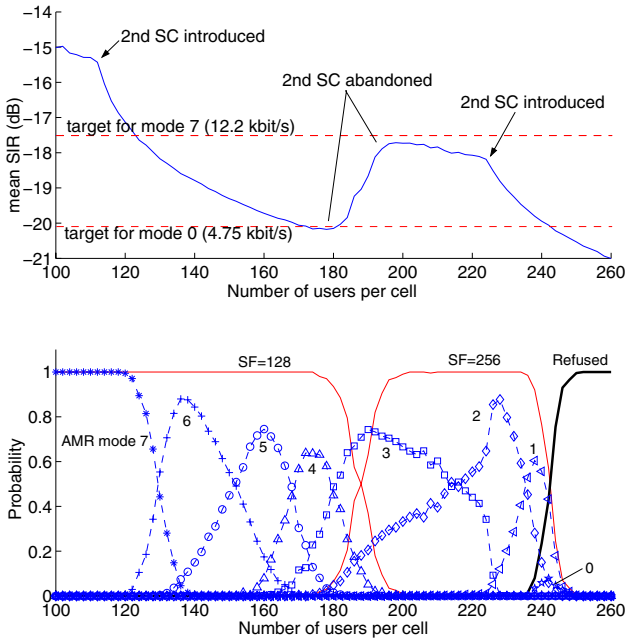


Figure 2: Downlink SIR; SF and AMR modes ($\alpha = 0.05$)

balanced SIR can result in the ability for some MSs to use AMR mode $n+1$, while all others can still remain at mode $n$.

When only few active MSs are present (less than 120), the SIR remains well above the target level. As the cell traffic grows (120. . . 180 users), the data rate per MS (i.e., the AMR mode) is reduced to increase transmission robustness under the influence of rising interference levels. The data rates of the selected AMR modes allow spreading factors of up to 128. SF=128 is chosen to accommodate as many users as possible within one OVSF tree, but if the capacity of one tree is exceeded, a second tree with a different scrambling code is employed, resulting in increased intra-cell interference.

As the decreasing SIR value forces the AMR codec to be used in its lowest modes, a higher spreading factor of 256 can be chosen. This approximately doubles the number of users within one OVSF tree, and thereby disbands the need for a second scrambling code. A source of intra-cell interference disappears and rising SIR values indicate an increasing transmission quality.

## 3. RRM STRATEGIES WITH MACRODIVERSITY

The simulator described in the previous section is extended for the following simulations with macrodiversity and Rayleigh fading [6]. The graphical output of the system-level simulator illustrates a network with MSs and BSs in an area of, e.g., 2.5 × 2.5 km. The positions of the MSs and BSs, which are depicted as dots and squares, respectively, are determined by the user. A macrodiversity map shows the cells in the surrounding of the BSs and their overlap in the macrodiversity areas. This simulator is used to examine different RRM strategies with macrodiversity and to observe the behavior of a UMTS network for various traffic situations.

With macrodiversity, the Radio Resource Management (RRM) [2] has to provide the signal to the correct base stations for the downlink direction and to handle the power partitioning between the different links from the base stations to the mobile station. In the context of macrodiversity, one reasonable goal of the RRM strategies is a balanced traffic load of all BSs. Different RRM strategies considering macrodiversity are presented and examined here. As a side effect, these strategies reduce negative effects on the capacity of the UMTS system.

### 3.1. Negative Effects on Capacity

Two system-immanent effects with negative impact on the capacity are described in this subsection. Fig. 3 shows two cells and the mobile station $\mathrm{MS}_j$ in the middle between the base stations $\mathrm{BS}^0$ and $\mathrm{BS}^1$. The left-hand cell contains many mobiles causing intense traffic. In contrast, the right-hand cell is nearly empty. At the beginning of the scenario, $\mathrm{MS}_j$ wants to establish a radio link to the BS with the lowest interference. $\mathrm{MS}_j$ calculates the SIR of the pilot channel of $\mathrm{BS}^0$ in the case of $\alpha = 0$:

$$\mathrm{SIR}^0 = \frac{P_j^{0,\mathrm{pilot}}}{P^{1,\mathrm{signal}} + P_j^{1,\mathrm{pilot}}} \tag{15}$$

with the pilot channel power $P_j^{0,\mathrm{pilot}}$ of $\mathrm{BS}^0$, the interference power of the other BS's pilot channel, $P_j^{1,\mathrm{pilot}}$, and the total interference power $P^{1,\mathrm{signal}}$ from $\mathrm{BS}^1$ to the MSs in the neighboring cell excluding the pilot power. The $\mathrm{MS}_j$ also calculates the pilot channel SIR of $\mathrm{BS}^1$ with the same Eq. 15 but exchanged indices 0 and 1.

Assuming that the pilot channel powers are equal in both cells, perfect orthogonality of the OVSF codes with $\alpha = 0$, and that both BSs use only one scrambling code each, $\mathrm{SIR}^0$ and $\mathrm{SIR}^1$ differ only by the interference power $P^{1,\mathrm{signal}}$. If the MS in the center of the two BSs logged on to the right-hand $\mathrm{BS}^1$, the MS would receive the interference from all mobiles in the left-hand cell due to the different scrambling codes used in the two adjacent cells. However, if the MS logged on to the left-hand $\mathrm{BS}^0$, only the few mobiles in the right-hand cell would cause interference. As a result, the MS in the middle of the BSs measures $P^{0,\mathrm{signal}} \gg P^{1,\mathrm{signal}}$ due to the different traffic load and connects to $\mathrm{BS}^0$. This means an expansion of the cell of $\mathrm{BS}^0$ and a reduction of the cell of $\mathrm{BS}^1$ (Fig. 3). The high traffic load of $\mathrm{BS}^0$ is increased, and the capacity of $\mathrm{BS}^1$ remains unused.

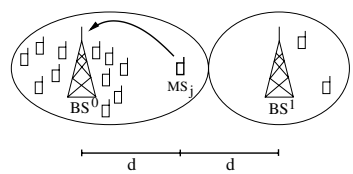


Figure 3: MS in the center between two BSs connects to the full cell with $\mathrm{BS}^0$.

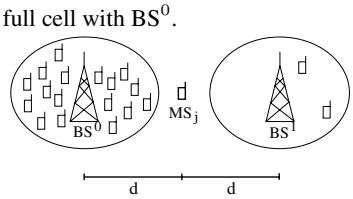


Figure 4: MS drops both the connections to $\mathrm{BS}^0$ and to $\mathrm{BS}^1$, and loses radio coverage completely.

The cell breathing in UMTS causes another effect contrary to a balanced traffic load of all BSs and to a high system capacity. We again assume two neighboring cells with a mobile station placed in the middle between the two BSs. At first, $\mathrm{MS}_j$ is connected to both base stations with a low traffic load. Then, we assume that due to increasing traffic more and more mobiles are connected to the left-hand $\mathrm{BS}^0$. The emitted power of $\mathrm{BS}^0$ increases and causes interference. The scrambling code of $\mathrm{BS}^0$ disturbs the connection of the $\mathrm{BS}^1$ to $\mathrm{MS}_j$ with the high emitted power of $\mathrm{BS}^0$. As a result, the cell of $\mathrm{BS}^1$ becomes smaller. MSs at the cell border of the right-hand cell cannot hold the connection to $\mathrm{BS}^1$ due to the high interference power from $\mathrm{BS}^0$ (Fig. 4).

In the further progress of traffic increase, $\mathrm{BS}^0$ has to use a second scrambling code to accommodate all connection requests of

the MSs in the left-hand cell. However, with the second scrambling code the intra-cell interference increases, the left-hand cell becomes smaller (Fig. 4). Especially MSs at the cell border lose their radio link to $BS^0$. In consequence, $MS_j$ between $BS^0$ and $BS^1$ has lost both connections and is not covered any more. Between the two neighboring cells, an area without radio coverage has emerged. The size of the cell of $BS^1$ has changed, although its pilot power remains the same during the whole scenario.

### 3.2. Power Partitioning

We introduce a specific power partitioning mechanism to balance the traffic load and therewith to balance the transmitted powers of all BSs in the network, and describe its effect on the capacity. With this mechanism, the RRM can avoid cell overload, and extreme interference peaks. The power transmitted to a specific $MS_j$ by, e.g., two base stations $BS^0$ and $BS^1$ can be subdivided with this control mechanism into all possible ratios $P_j^0/P_j^1$, not necessarily $P_j^0/P_j^1 = 1$. The power partitioning algorithm exploits the total powers of the BSs to determine the distribution of the powers transmitted on the different links to $MS_j$ in the macrodiversity area.

Each connection of a $BS^i$ to a specific $MS_j$ is provided with an index value in the range from 1 to 100 calculated with the following equation:

$$\text{Power-Index}_{BS^i \to MS_j} = \begin{cases} 1 & \text{for } P^i > P^{\text{average}} + P^{\text{tolerance}} \\ 100 & \text{for } P^i < P^{\text{average}} - P^{\text{tolerance}} \\ \left(\frac{P^{\text{average}} - P^i}{P^{\text{tolerance}}} \cdot 50\right) + 50 & \text{else} \end{cases} \tag{16}$$

The RRM searches the two BSs with the minimum and the maximum power out of all BSs in the local area. The average $P^{\text{average}}$ of these two values is calculated. The total power of $BS^i$, $P^i$, is subtracted from $P^{\text{average}}$. The result is the distance between $P^i$ and the target power value for all BS, $P^{\text{average}}$.

The distance value is then normalized with $P^{\text{tolerance}}$. This tolerance value determines the maximum difference between a BS power and the average BS power $P^{\text{average}}$ in which the power partitioning algorithm controls the power sharing between the BSs and the specific $MS_j$ in a linear way (Fig. 5). The result is then mapped onto the Power-Index$_{BS^i \to MS_j}$ for the link from $BS^i$ to $MS_j$. If $P^i$ is greater (smaller) than the sum (difference) of $P^{\text{average}}$ and $P^{\text{tolerance}}$, the lowest (highest) power index 1 (100) is assigned to $BS^i$ (Fig. 5). If a BS emits more (less) total power than $P^{\text{average}}$, its power transmitted to $MS_j$ is reduced (increased) by the RRM.

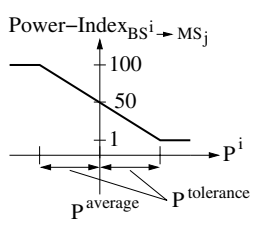


Figure 5: Assignment of a power index to BS power

The choice of $P^{\text{tolerance}}$ is significant for the power partitioning algorithm. If this value is too low, the goal of balanced BS powers cannot be reached, because extreme differences between the powers on the downlink connections to $MS_j$ occur. If $P^{\text{tolerance}}$ is too high, the impact of the power partitioning algorithm is reduced due to the larger distance which has to be covered by the index values from 1 to 100 (Fig. 5), and a fine tuning is impossible. In our scenarios we set $P^{\text{tolerance}}$ empirically to, e.g., 4 W, if the maximum BS power is set to 10 W.

All power indices of the connections to $MS_j$ are converted into percental values which are multiplied with the total power desired by $MS_j$ to obtain the power target value of each connection. The RRM ensures that the new power targets are achieved by the BSs. This algorithm is repeated with all MSs in the macrodiversity areas of the system.

### 3.3. Pilot Power Control

The power partitioning mechanism for macrodiversity areas is combined with the pilot power control. The pilot power control determines the size of the cell and of the macrodiversity area. An RRM strategy for balancing the power of all BS should reduce the pilot power of heavily loaded cells and increase it in less loaded neighboring cells. Thus, overload of cells and gaps due to cell breathing can be reduced; the number of active users is increased. This control mechanism influences the downlink connections only indirectly and its impact on the capacity depends on the distribution of the mobile stations.

### 3.4. Simulation Results

In our scenarios for the downlink, the power received by each MS is not increased by macrodiversity. All simulations were executed with the system-level simulator assuming a 15 kbit/s speech service with SF=256, omnidirectional antennas, propagation path loss and optional Rayleigh fading, and an AWGN channel.

The areas without coverage, which can arise by the cell breathing, are reduced by the presented RRM strategies with macrodiversity. In addition, the capacity of a single cell can be increased, if the MSs at the cell boundary are additionally connected to the base stations in the neighborhood. In this case, the BS of the single cell needs less power to reach the MSs in the macrodiversity area.

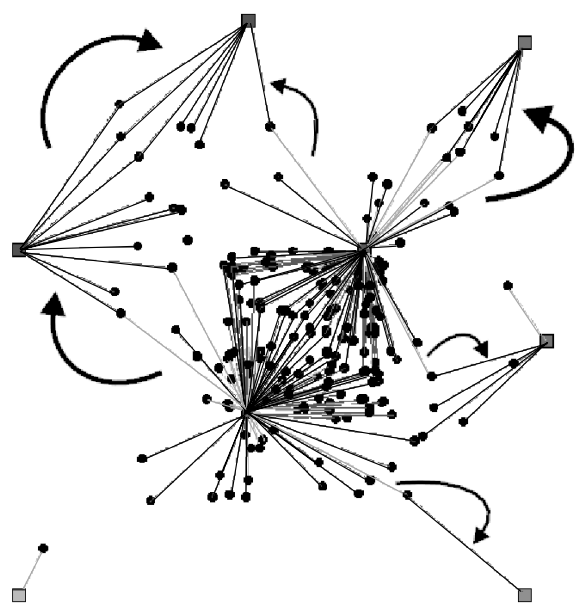

Figure 6: Power drifting by power partitioning: relief of the overloaded area by neighboring cells (MSs: dots; BSs: squares; connections: lines)

Our statistical system-level simulations confirm the increase of the cell capacity by the presented RRM strategies: In our scenario, the total emitted power of a heavily loaded BS with, e.g., 175 mobile stations is reduced with the power partitioning algorithm. This reserve can be used to take in another 28 mobile stations. Fig. 6 shows the scenario in a plot from the system-level simulator with 203 MSs (dots) altogether, and 8 BSs (squares) distributed in an area of approx. 2.5 $\times$ 2.5 km. The different powers

of the BSs and of the downlink connections (lines) are depicted by different greyscales: Light greyscales indicate low power and dark greyscales high power. In the center of Fig. 6, an area with a high density of MSs (dots) is depicted. The two BSs (squares) providing radio coverage for this area have to be relieved by the neighboring cells. The power partitioning algorithm of the RRM ensures a power drifting for the MSs in the macrodiversity areas from the overloaded BSs to the neighboring BSs with less traffic load, which are again relieved by their neighboring cells. An example for the latter effect is marked by the arrow in the top left-hand corner of Fig. 6.

In another scenario with 270 mobile stations within 8 cells and 30 MSs without radio coverage, the pilot power control leads to a reduction of the gaps between the cells. As a result, 24 out of the 30 MSs are connected to a BS. The remaining 6 MSs could not be covered, because with the increasing pilot power the interference level is increased, too. In consequence, a further increase of the pilot power does not lead to an additional capacity gain.

| Scenario | #MS | $\#MS_{no\ link}$ | $\#MS_{no\ link}$,fad. |
|---|---|---|---|
| 1 no macrod., no RRM | 220 | 1 | 54 |
| 2 macrod., no RRM | 220 | 2 | 57 |
| 3 macrod. + RRM | 242 | 0 | 47 |

Table 1: Simulation results: example with 8 BSs

Table 1 shows an example of the simulation results. The second column indicates the total number of MSs in the system. The last two columns give the total number of unconnected MSs without (third column) and with Rayleigh fading (fourth column). The scenarios 1 and 2 are simulated without and with macrodiversity, but without any RRM strategies. The slightly worse results in the case of macrodiversity are caused by MSs at the border of a cell. They are not connected because of the additional interference due to additional connections in the macrodiversity area.

In scenario 3 power partitioning and pilot power control are simulated together. With these two RRM strategies, 22 additional MSs can be linked to a BSs, and the number of MSs without radio coverage is diminished significantly.

## 4. CONCLUSIONS

The presented scrambling code allocation method was shown to enhance the cell capacity in a UMTS-FDD system. The improvement was derived analytically by maximizing the mean SIR in an idealized cell environment. Statistical simulations confirm our theoretical results.

With the presented RRM strategies taking macrodiversity into consideration, the capacity of a single cell can be increased, e.g., in the case of short-term overload. The size of macrodiversity areas can be adjusted to a certain extent by the pilot power control mechanism. Thus, the power resources of less loaded cells can be exploited more efficiently by power partitioning. This is an important feature for cells which are overloaded only in specific rare situations. The wireless network does not have to be designed for the case of a very high traffic load, because a high amount of MSs can be covered with the help of the RRM strategies presented in this paper. Our simulation results indicate an additional capacity gain by the combination of the proposed RRM strategies.

## REFERENCES


[1] 3rd Generation Partnership Project (3GPP), "Universal Mobile Telecommunications System (UMTS), Rel. 99: TS 25.101, TS 25.213, TS 25.922,"

[2] N. D. Tripathi, J. H. Reed and H. F. VanLandingham, *Radio Resource Management in Cellular Systems*. Kluwer Academic Publishers, 2001.

[3] H. Holma and A. Toskala, *WCDMA for UMTS*. John Wiley & Sons, Ltd., 2000.

[4] Wan Choi and Jin Young Kim, "Forward-Link Capacity of a DS/CDMA System with Mixed Multirate Sources," IEEE Transactions on Vehicular Technology, May 2001.

[5] Duk Kyung Kim and Dan Keun Sung, "Capacity Estimation for a Multicode CDMA System with SIR-Based Power Control," IEEE Transactions on Vehicular Technology, May 2001.

[6] J. Trenzinger, "Effect of Macrodiversity on the Capacity of the UMTS Mobile Communication System," Diploma Thesis (in German), Institute of Communication Systems and Data Processing, RWTH Aachen, 2001.